THE JOURNAL OF BIOLOGICAL CHEMISTRY VOL. 284, NO. 4, pp. 2169–2175, January 23, 2009


# A Comprehensive Model for Packing and Hydration for Amyloid Fibrils of $\beta_2$-Microglobulin*[S]

Received for publication, September 8, 2008, and in revised form, November 10, 2008 Published, JBC Papers in Press, November 18, 2008, DOI 10.1074/jbc.M806939200

**Young-Ho Lee[‡], Eri Chatani[‡], Kenji Sasahara[‡], Hironobu Naiki[§], and Yuji Goto[‡1]**

*From the [‡]Institute for Protein Research, Osaka University and CREST, Japan Science and Technology Agency, 3-2 Yamadaoka, Suita, Osaka 565-0871 and [§]Faculty of Medical Sciences, University of Fukui, and CREST, Japan Science and Technology Agency, Fukui 910-1193, Japan*

**Volume can provide informative structural descriptions of macromolecules such as proteins in solution because a final volumetric outcome accompanies the exquisite equipoise of packing effects between residues, and residues and waters inside and outside proteins. Here we performed systematic investigations on the volumetric nature of the amyloidogenic conformations of $\beta_2$-microglobulin ($\beta$2-m) and its amyloidogenic core peptide, K3, using a high precision densitometer. The transition from the acid-denatured $\beta$2-m to the mature amyloid fibrils was accompanied by a positive change in the partial specific volume, which was larger than that observed for the transition from the acid-denatured $\beta$2-m to the native structure. The data imply that the mature amyloid fibrils are more voluminous than the native structure because of a sparse packing density of side chains. In contrast, the formation of the mature amyloid-like fibrils of the K3 from the random coil was followed by a considerable decrease in the partial specific volume, suggesting a highly compact core structure. Interestingly, the immature amyloid-like fibrils of $\beta$2-m exhibited a volume intermediate between those of the mature fibrils of $\beta$2-m and K3, because of the core structure at their center and the relatively noncompact region around the core with much hydration. These volumetric differences would result from the nature of main-chain-dominated fibrillogenesis. We suggest comprehensive models for these three types of fibrils illustrating packing and hydrational states.**

A polypeptide chain folds spontaneously to the most stable form, the native structure. However, it has been recognized that a misfolding-induced ordered aggregate, known as an amyloid, is an alternative fold that might be in the global minimum of free energy (1). Intriguingly, various nonamyloidogenic polypeptides can also assemble into fibrillar structures, implying that fibrillation is a generic property of polypeptides (2). This raises the possibility that although the native structure depends on interactions among side chains of amino acid residues, *i.e.* a side-chain-dominated structure, the amyloidogenic structure does not depend on interactions of side chains, *i.e.* a main-chain-dominated structure. It is therefore conceivable that a main-chain-dominated fibrillar structure is misfolded without optimal packing of side chains, and a side-chain-dominated native structure has evolved pursuing a unique fold with optimal packing of residues (3–6). This defective packing results in a lot of cavities, thereby rendering multiple fibrillar conformations, the so-called polymorphism (4). By contrast, fibrils of amyloidogenic core peptides were suggested to possess tight packing (7–12) that could constitute the core structure of the fibrils made of whole protein accommodating this peptide.

Although the past decade has seen progress in our biophysical understanding of amyloid fibrils using various approaches (3, 4, 6–16), much remains to elucidate about the conformational and thermodynamic features of fibrous proteins. In this respect, the volumetric technique for fibrillogenesis is a promising alternative, because volume is a key thermodynamic quantity and can sensitively probe changes of molecular hydration (17), intrinsic packing (18), and dynamics (19) upon conformational transitions and molecular binding events such as protein (un)folding and formation of aggregates in solution (20).

Indeed, although there have been a few studies of the volume of fibrils (3, 21–25), there is no consensus over the volumetric properties of fibrillation. Our previous study (3) showed that mature amyloid fibrils of $\beta_2$-microglobulin ($\beta$2-m)[2] (99 residues) are in a voluminous state with loose packing. Similarly, Foguel *et al.* (21) reported that amyloidogenesis of transthyretin (TTR, 127 residues) and $\alpha$-synuclein (140 residues) correlated with less packed structures (larger volume changes). Akasaka *et al.* (22) also found that a disulfide-deficient variant of hen egg white lysozyme (HEWL, 129 residues) formed flexible amyloid-like fibrils with an increase in volume. Conversely, Winter and co-workers (23, 24) observed that the transition from poly-D-lysine (~200 residues) and insulin (51 residues) monomers to mature fibrils was in both cases accompanied by reductions in volume (*i.e.* structural compaction). It is also intriguing that the mature and the early fibrils of a short fragment of TTR-(105–115) (11 residues) take denser and looser packing than the mature fibrils of full-length TTR, respectively (21, 25). These disparities of volumetric changes on fibrillation

* This work was supported by the Japanese Ministry of Education, Culture, Sports, Science, and Technology (to Y. G.) and by the Japan Society for Promotion of Science postdoctoral fellowship (to Y.-H. L.). The costs of publication of this article were defrayed in part by the payment of page charges. This article must therefore be hereby marked "*advertisement*" in accordance with 18 U.S.C. Section 1734 solely to indicate this fact.

[S] The on-line version of this article (available at http://www.jbc.org) contains additional Experimental Procedures, Figs. S1 and S2, and additional references.

[1] To whom correspondence should be addressed. E-mail: ygoto@protein.osaka-u.ac.jp.

[2] The abbreviations used are: $\beta$2-m, $\beta_2$-microglobulin; ASA, accessible surface area; AUC, analytical ultracentrifugation; AFM, atomic force microscopy; Gdn-HCl, guanidine hydrochloride; $HD_{ex}$, hydrogen deuterium exchange; PMV, partial molar volume; SV, sedimentation velocity; ThT, thioflavin T; HEWL, hen egg white lysozyme; TTR, transthyretin.

could reflect the intrinsic feature of polymorphism of amyloid(-like) fibrils.

Most importantly, to obtain a reliable volume value of a solute of interest, one should certify that solutes are dispersive enough without precipitation (17) and confirm the constituent components with their populations. These prerequisites become more serious in the case of a polymerization reaction such as fibrillation. Fibrillar or amorphous aggregates are apt to precipitate because of high molecular weight, and unreacted monomers are often left.

In view of the notions for the polymorphism and core structures of fibrils, the model of the amyloidogenicity of β2-m is excellent because volumetric properties of the various fibrillar structures formed by the identical β2-m and its fragment can be examined systematically. Typically, rigid and long amyloid fibrils referred to as "mature fibrils" are assembled by acid-denatured β2-m (3–5, 16, 26). At high concentrations (>200 mM) of sodium chloride at acidic pH, β2-m can assemble spontaneously into flexible thin amyloid-like fibrils, often called "immature fibrils" (26, 27). In addition, K3 peptide, an amyloidogenic core fragment corresponding to Ser-20 to Lys-41 of β2-m, can form amyloid-like fibrils similar to mature fibrils at neutral pH (14) and thin filamentous fibrils at acidic pH in the absence and presence of 20% (v/v) 2,2,2-trifluoroethanol, respectively (28).

Keeping the prerequisites for preparing sample solution for densitometry described above in mind and to gain insight into volumetric properties of amyloidogenesis, we have performed direct measurements of changes in volume accompanying the fibrillation of β2-m and K3, using a high precision densitometry. To our surprise, the extent of the partial volumetric changes upon the formation of the mature fibrils and immature fibrils of β2-m, and the mature fibrils of K3, differed. Here we report the partial volume and states of these three fibrillar conformations in light of the main-chain-dominated fibrillation and the core structure of fibrils with polymorphism.

## EXPERIMENTAL PROCEDURES

*Preparation and Characterization of the Samples*—Recombinant human β2-m was expressed and purified using the *Escherichia coli* expression system as described (15). K3 was obtained by digestion of β2-m with lysyl endopeptidase (*Achromobacter* protease I) as reported (16). For CD and measurements of density, β2-m was dissolved in 6 mM HCl (pH 2.3) and 38 mM NaCl or 50 mM citrate buffer (pH 2.5) in the presence and absence of 5.7 M Gdn-HCl and, in turn, K3 in solution of 6 mM HCl and 38 mM NaCl. Mature β2-m fibrils of 1.2 mg·ml$^{-1}$ were elongated in a 6 mM HCl solution (pH 2.3) containing 38 mM NaCl in the presence of 5 μg·ml$^{-1}$ of seeds, ultrasonicated fibrils, at 37 °C for ~14 h. The short mature fibrils were prepared by ultrasonicating the fresh mature fibrils 100 times on ice using a Microson sonicator (Misonix, Farmingdale, NY) at intensity level 2 and with 20 1-s pulses. The fibrils were confirmed to be fragmented with AFM (data not shown). Immature fibrils of β2-m were spontaneously polymerized as reported (26) in a reaction mixture containing 0.6 mg·ml$^{-1}$ of recombinant β2-m, 50 mM citrate buffer (pH 2.5), and 200 mM NaCl. The reaction solution was incubated at 37 °C for ~90 h. Mature fibrils of K3 were seed-dependently polymerized by K3 monomer in the solution

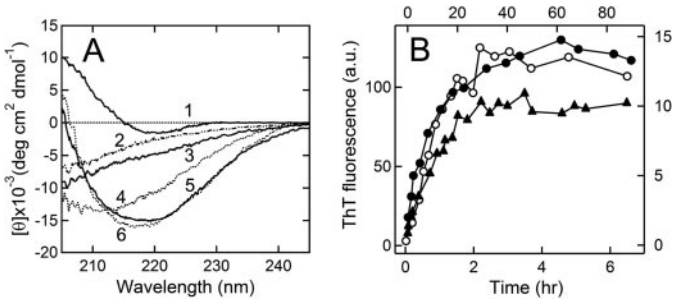


FIGURE 1. **Conformational characterization and formation of fibrils.** *A*, far-UV CD spectra for the different structures of β2-m and K3 peptide were obtained. *1*, native β2-m; *2*, K3 peptide; *3*, acid-denatured β2-m; *4*, immature fibrils of β2-m; *5*, mature fibrils of β2-m; and *6*, mature fibrils of K3. *B*, formation of the three types of fibrils was monitored by ThT fluorescence. The intensity of ThT for the mature β2-m fibrils (○) and both the immature β2-m fibrils (▲) and the mature K3 fibrils (●) was plotted against incubation time on the *lower* and *upper axes*, respectively. The *left* and *right axes* are corresponding to the intensity of ThT of the mature β2-m fibrils and the other fibrils, respectively.

containing 6 mM HCl, 7 mM NaCl, and 0.00091% 2,2,2-trifluoroethanol. Details of the preparation of K3 fibrils are presented in the supplemental material. All the polymerization reactions in this study were traced by fluorometric analysis using ThT and monitored at 485 nm with excitation at 445 nm with a Hitachi fluorescence spectrophotometer, F4500, at 25 °C as reported (16, 26). Far-UV CD spectra of all samples were measured at 25 °C with a Jasco J-600 spectropolarimeter, using a cell with a light-path of 1 mm. AFM images were obtained using a Nano Scope IIIa (Digital Instruments/Veeco) at 25 °C.

*Sedimentation Velocity (SV) with Analytical Ultracentrifugation (AUC)*—SV measurements were performed on the mature and immature fibrils of β2-m and the mature fibrils of K3 at 5 °C using a Beckman-Coulter Optima XL-1 analytical ultracentrifuge (Fullerton, CA) equipped with an An-60 rotor and two- or six-channel charcoal-filled Epon cells. After pre-centrifugation at 700 × *g* for 5 min, the rotor speed was increased to 17,400–31,000 × *g*. The sedimentation curves were recorded using absorbance data at 280 nm at intervals of 10–20 min. All conditions for SV were identical to those for polymerization reactions except temperature. Each measurement was conducted with a radial increment of 0.003 cm in a continuous scanning mode.

*High Precision Density Measurements*—All measurements of density were made using a vibrating tube density meter (DMA5000, Anton Paar, Austria) with a precision of 1 × 10$^{-6}$ g·ml$^{-1}$, and the polypeptide concentration was between 0.25 and 4 mg·ml$^{-1}$. To prevent condensation in measuring density at 5 °C, a U-shaped densitometric cell was thoroughly dried with the use of a dry air pump, and ambient relative air humidity and temperature were kept under 30% and 25 °C, respectively. The adjustments with water and air were performed following every single set of measurements, and almost no deviation of water density before and after a series of density measurements was confirmed.

## RESULTS

*Characterization of Various Conformational States*—The far-UV CD spectrum of native β2-m at pH 7.0 (Fig. 1*A*) is con-

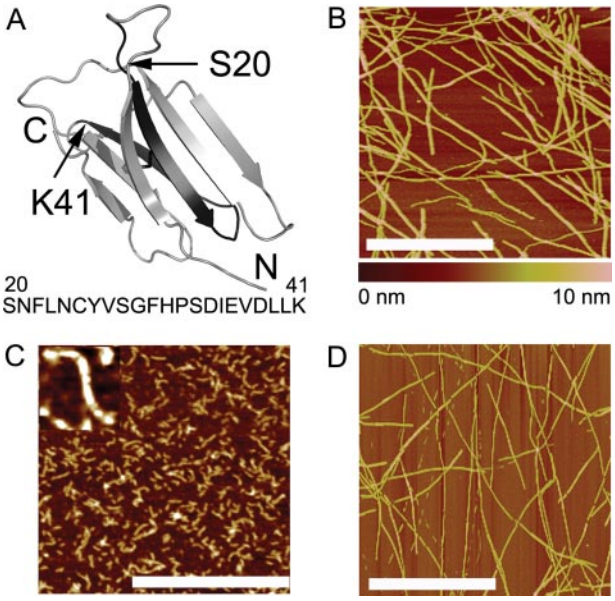


FIGURE 2. **Distinct conformational states of β2-m.** *A,* structure of native β2-m and amino acid sequence of K3 peptide. The region corresponding to the K3 is shown in *dark gray*. The three-dimensional structure was drawn by PyMOL (38) with the crystal structure (Protein Data Bank entry 2d4f) (15). AFM images of mature fibrils of β2-m (*B*), immature fibrils of β2-m (*C*), and mature fibrils of K3 (*D*) are shown. *C*, *inset*, curved immature fibrils are magnified. The *scale bars* represent 1 μm.

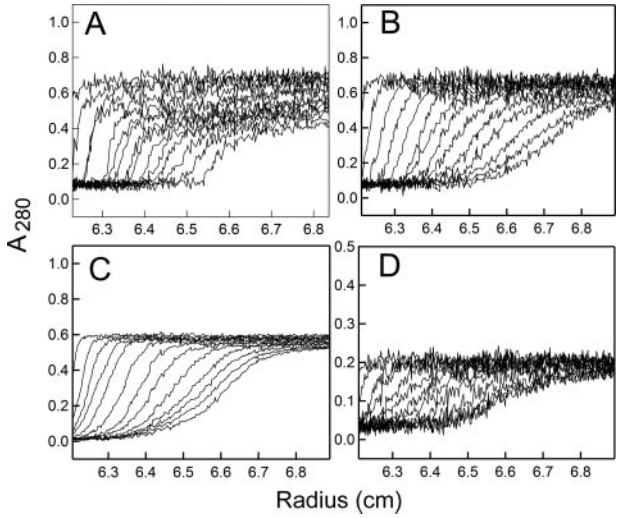


FIGURE 3. **Sedimentation velocity analyses of the fibrils of β2-m and K3.** The sedimentation curves of mature fibrils of β2-m (*A*), short mature fibrils of β2-m (*B*), immature fibrils of β2-m (*C*), and mature fibrils of K3 (*D*) were obtained at 5 °C by monitoring the absorbance at 280 nm.

sistent with that of our earlier study that exhibited a 7-stranded β-sheet as shown by x-ray crystallography (Fig. 2*A*) (15, 26). In contrast, β2-m is largely unfolded at pH 2.3 as indicated by far-UV CD (Fig. 1*A*).

We obtained a clear solution of the mature fibrils of β2-m by performing seed-dependent elongation in 6 mM HCl (pH 2.3) and 38 mM NaCl. The intensity of the ThT fluorescence increased with the incubation period without a lag time (Fig. 1*B*). The far-UV CD spectra of these fibrils possessed a minimum at 220 nm and were compatible with those of mature fibrils studied previously (Fig. 1*A*) (16, 26). In AFM images, mature fibrils showed a morphology similar to that of the typical amyloid fibrils formed at acidic pH and 100 mM NaCl, *i.e.* several micrometers in length with a diameter of ~5 nm (Fig. 2*B*) (3).

We ensured the satisfactory dispersion of fibrils for measurements of density and confirmed the presence of residual monomers using SV at 17,400 × *g* and 5 °C for several hours with AUC equipped with a UV-visible absorption optical system. We obtained a series of sedimentation curves by monitoring absorbance at 280 nm, suggesting the absence of precipitates, *i.e.* uniformly dispersed solutes (Fig. 3*A*). If much larger molecules not suitable for densitometric measurements are present, one cannot obtain a series of well defined sedimentation curves. For instance, amyloid β-(1–40) fibrils formed at pH 7.2 rapidly sedimented during pre-centrifugation at 700 × *g* within 5 min, as shown in supplemental Fig. S1*A*. On the basis of SV, a distribution of sedimentation coefficient ($s_{20,w}$) values for mature β2-m fibrils was obtained (supplemental Fig. S1*B*). The $s_{20,w}$, which reflects a molecular weight, showed a broad distribution from 100 S to 350 S. The variance in $s_{20,w}$ values may come from the difference in length of fibrils. The base lines of UV spectra of the sedimentation curves were slightly above zero, indicating that not all monomers transformed into fibrils. The residual monomers accounted for up to about 10% of the total intensity of absorbance.

To examine the effects on volume of the increase in accessible surface area (ASA) of the terminal parts of the fibrils, we further investigated the partial volume of short mature fibrils of β2-m prepared by ultrasonicating long mature fibrils. SV measurements for the short mature fibrils were conducted at 17,400 × *g* and 5 °C for several hours. We obtained a sedimentation pattern indicating the fibrils to be well dispersed (Fig. 3*B*). The $s_{20,w}$ values of short fibrils exhibited a narrow distribution from 50 S to 90 S (supplemental Fig. S1*B*). The values were smaller than those of long fibrils, implying that the fibrils were shortened by sonication. About 10% of residual monomers remained unreacted based on the absorbance at 280 nm (Fig. 3*B*).

The immature fibrils of β2-m were spontaneously polymerized in solution containing 200 mM NaCl at pH 2.5 and 37 °C. The formation of fibrils was monitored by the changes in intensity of ThT, and immature fibrils were elongated without a lag time as in our previous study (Fig. 1*B*) (26). The far-UV CD spectrum was consistent with that of the earlier study (Fig. 1*A*) (26). The AFM image revealed fibrils that were curved and short with a small diameter (~2 nm) (Fig. 2*C*). The immature fibrils prepared here were shorter than the previously reported immature fibrils (26) because of the low concentration of salt (200 mM NaCl) compared with the previous study (400 mM NaCl) (1). However, this difference could not affect volumetric properties as in the case of long and short mature fibrils of β2-m (see under "Discussion"). Based on the results of the SV experiments with AUC at 31,000 × *g* and 5 °C for several hours, immature fibrils were in a sufficiently dispersed state (Fig. 3*C*). The $s_{20,w}$ values showed a narrow distribution from 10 S to 30 S (supplemental Fig. S1*B*). The smaller $s_{20,w}$ values than those of mature fibrils would be due to the short length and single-stranded property (Fig. 2*C*). The base lines of UV spectra were

nearly zero, indicating that almost all monomers were transformed into fibrils (Fig. 3*C*).

The far-UV CD spectrum of K3 peptides at 6 mM HCl (pH 2.3) and 38 mM NaCl showed a substantially unfolded structure (Fig. 1*A*). The mature fibrils were seed-dependently polymerized at 6 mM HCl (pH 2.3) and 7 mM NaCl. The fibril formation monitored by ThT intensity exhibited a similar profile to that of immature fibrils but was slightly higher (Fig. 1*B*). The CD spectrum of K3 fibrils was similar with that of mature β2-m fibrils (Fig. 1*A*). The AFM image of K3 fibrils revealed long thin fibrillar structures with a diameter of ~3 nm (Fig. 2*D*). SV experiments were also undertaken at 17,400 × *g* and 5 °C for several hours. We found that mature K3 fibrils were dispersive enough, and about 10% K3 monomers were left as judged from absorbance baselines (Fig. 3*D*). The distribution of $s_{20,w}$ values of K3 fibrils had a broad range from 10 S to 120 S (supplemental Fig. S1*B*). Considering the long length of K3 fibrils (Fig. 2*D*), the small $s_{20,w}$ values compared with those of β2-m fibrils could result from the low molecular weight of K3 monomers and the single- or double-stranded property.

*Density and Volumetric Measurements*—Density values of individual samples measured were transformed into the apparent specific volume ($\nu_{app}$) using Equation 1. To obtain the partial specific volume at infinite dilution, $\nu^\circ$, a series of $\nu_{app}$ values were plotted against concentration and then linearly extrapolated to the zero concentration according to Equation 2 (Fig. 4),

$$\nu_{app} = 1/c - (\rho - c)/\rho_0 c \quad \text{(Eq. 1)}$$

$$\nu^\circ = \lim_{c \to 0} \nu_{app} \quad \text{(Eq. 2)}$$

where $\rho$ and $\rho_0$ are the densities of the solution and solvent, respectively; and $c$ is the specific concentration of the protein in grams/ml of solution. The measured densities and calculated $\nu_{app}$ of all the samples are shown in Fig. 4, and the mean $\nu^\circ$ values of the three series of density measurements for all the samples are presented Table 1.

The $\nu^\circ$ values of several native proteins, *i.e.* ferredoxin-NADP$^+$ reductase (FNR), ferredoxin, HEWL, and β2-m, varied depending on the kinds of proteins and the temperature. We first obtained a $\nu^\circ$ of HEWL comparable with that of an earlier study under the same conditions (29). The $\nu^\circ$ of FNR was larger than that of ferredoxin at pH 6.0 and 20 °C. Native β2-m at pH 7.0 and 20 °C had a small $\nu^\circ$ compared with ferredoxin and FNR. The $\nu^\circ$ of native β2-m dropped as the temperature was lowered. For the densitometry of all fibrils prepared, we conducted measurements at low temperature, 5 °C, to avoid destabilization and lateral aggregation of fibrils. Hence, to compare differences in the volume of diverse conformational states at the same temperature, the densities of native and denatured β2-m as well as K3 peptide were also measured at 5 °C. The $\nu^\circ$ values obtained were in the following order: mature fibrils > native monomer > acid-denatured monomer ≈ K3 monomer > immature fibrils ≫ mature fibrils of K3.

The formation of the main-chain-dominated structure of fibrils from monomers showed various changes in volume. Mature fibrils of β2-m showed the largest $\nu^\circ$ of the polypeptides explored here. The $\nu^\circ$ values of immature and mature K3 fibrils

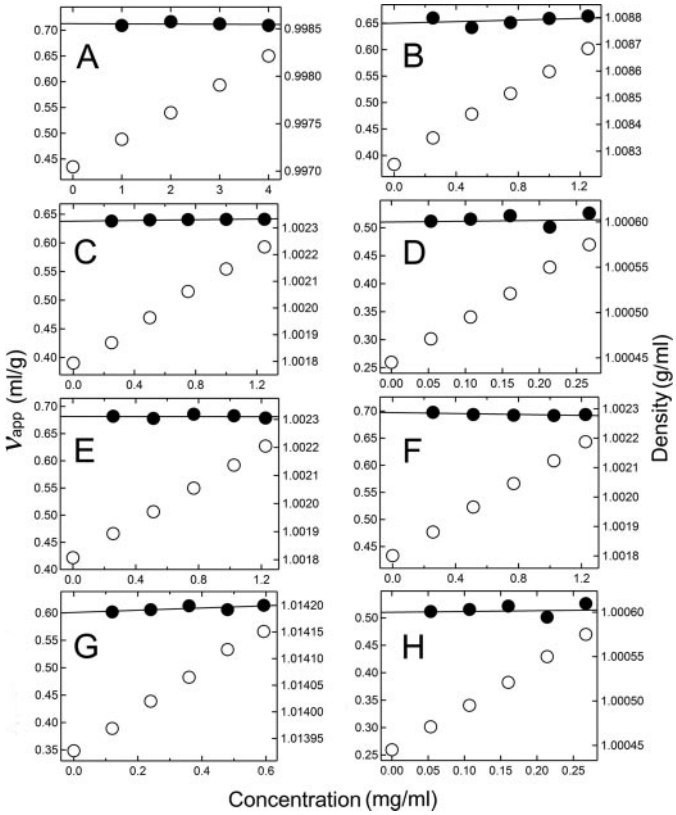


FIGURE 4. **Density and apparent specific volume ($\nu_{app}$) values for various conformational states of polypeptides.** *A–H,* measured densities (○) were plotted against concentration for HEWL (*A*), native β2-m (*B*), acid-denatured β2-m (*C*), K3 peptide (*D*), long mature fibrils of β2-m (*E*), short mature fibrils of β2-m (*F*), immature fibrils of β2-m (*G*), and mature fibrils of K3 peptide (*H*). The density measurements were conducted at 5 °C except for HEWL, which was measured at 25 °C. Individual density values of polypeptides were converted to $\nu_{app}$ (●) using Equation 1 and plotted as a function of concentration. To obtain partial specific volume at infinite dilution ($\nu^\circ$), $\nu_{app}$ values were linearly extrapolated to the zero concentration on the basis of Equation 2. One series of density and $\nu_{app}$ values of the three are shown. The *left* and *right axes* represent $\nu_{app}$ and density, respectively.

were lower than a side-chain-dominated native β2-m. The $\nu^\circ$ value of mature K3 fibrils was the lowest of the three fibrous conformations. As largely extended β2-m folded to its a native structure, the $\Delta\nu^\circ$ increased as much as 0.016 ± 0.009 ml·g$^{-1}$. This $\Delta\nu^\circ$ corresponds to the change in partial molar volume (PMV) of 190 ± 106 ml·mol$^{-1}$. The transition from the unfolded β2-m to mature fibrils was accompanied by an augmentation of volume, $\Delta\nu^\circ$ = 0.046 ± 0.008 ml·g$^{-1}$ and ΔPMV = 499 ± 108 ml·mol$^{-1}$. Interestingly, the formation of immature fibrils from the unfolded β2-m caused decreases in volume, $\Delta\nu^\circ$ = −0.044 ± 0.008 ml·g$^{-1}$ and ΔPMV = −523 ± 96 ml·mol$^{-1}$. The transition of K3 from a monomer to fibrils was followed by a much larger reduction in volume, $\Delta\nu^\circ$ = −0.137 ± 0.006 ml·g$^{-1}$ and ΔPMV = −343 ± 16 ml·mol$^{-1}$. It should be noted that $\nu^\circ$ values of mature fibrils of β2-m and K3 were corrected on the basis of those of the unreacted monomers (10%).

## DISCUSSION

*Determinants of Changes in Volume*—The partial specific volume of a solute at infinite dilution, $\nu^\circ$, can be presented as the sum of four terms (Equation 3) (18, 19, 30, 31).

**TABLE 1**
**Summary of partial specific volume ($\nu^\circ$) for polypeptides of various conformations**

| Polypeptide | $\nu^\circ$ | Conditions |
|---|---|---|
| | *ml·g*$^{-1}$ | |
| Native HEWL | 0.711 ± 0.002 | 25 °C, water from this study |
| Native HEWL | 0.712 ± 0.001 | 25 °C, water from Gekko and Noguchi (29) |
| Native FNR | 0.709 ± 0.001 | 20 °C, 25 mM sodium phosphate (pH 6.0) and 50 mM $NaClO_4$ |
| Native ferredoxin | 0.686 ± 0.003 | 20 °C, 25 mM sodium phosphate (pH 6.0) and 50 mM $NaClO_4$ |
| Native β2-m | 0.668 ± 0.004 | 20 °C, 50 mM sodium phosphate (pH 7.0) and 38 mM NaCl |
| Native β2-m | 0.652 ± 0.004 | 5 °C, 50 mM sodium phosphate (pH 7.0) and 38 mM NaCl |
| Denatured β2-m | 0.640 ± 0.001 | 5 °C, 50 mM sodium citrate (pH 2.5) |
| Denatured β2-m | 0.620 ± 0.002 | 5 °C, 50 mM sodium citrate (pH 2.5) and 5.7 M Gdn-HCl |
| Denatured β2-m | 0.636 ± 0.008 | 5 °C, 6 mM HCl (pH 2.3) and 38 mM NaCl |
| K3 peptide of β2-m | 0.635 ± 0.006 | 5 °C, 6 mM HCl (pH 2.3) and 38 mM NaCl |
| Mature β2-m fibrils (long) | 0.682 ± 0.009 | 5 °C, 6 mM HCl (pH 2.3) and 38 mM NaCl |
| Mature β2-m fibrils (short) | 0.697 ± 0.013 | 5 °C, 6 mM HCl (pH 2.3) and 38 mM NaCl |
| Mature K3 fibrils | 0.498 ± 0.002 | 5 °C, 6 mM HCl (pH 2.3) and 7 mM NaCl |
| Immature β2-m fibrils | 0.596 ± 0.008 | 5 °C, 50 mM sodium citrate (pH 2.5) and 200 mM NaCl |

$$\nu^\circ = \nu_{geo} + \nu_{cav} + \Delta\nu_{hyd} + \nu_{therm} \quad \text{(Eq. 3)}$$

where $\nu_{geo}$ represents the geometric volume of the constituent atoms such as the van der Waals and excluded volumes, and $\nu_{cav}$ reflects the cavity (void) volumes in the interior of the molecule because of imperfect atomic packing. Thus increases in $\nu_{geo}$ or $\nu_{cav}$ serve as elevating the volume. $\Delta\nu_{hyd}$ indicates the changes in volume resulting from hydration of the molecule and can be divided into three terms, the hydration of apolar ($^{apol}\nu_{hyd}$), polar ($^{pol}\nu_{hyd}$), and charged ($^{cha}\nu_{hyd}$) atomic groups. $^{pol}\nu_{hyd}$ and $^{cha}\nu_{hyd}$ contribute negatively to $\Delta\nu_{hyd}$ because of hydrogen bonding or electrostriction (18, 19, 30). Although there is the report of the positive contribution of $^{apol}\nu_{hyd}$ to $\Delta\nu_{hyd}$, the sign of $^{apol}\nu_{hyd}$ is still controversial (32). $\nu_{therm}$ refers to thermal volume that represents the void space around the solute molecules that arises from the mutual thermal motions of the solute and solvent molecules (18, 19, 30), and contributes positively to changes in volume.

It should be noted that increasing the ASA is closely related to increasing $\nu_{geo}$, $\nu_{hyd}$, and $\nu_{therm}$. It is generally accepted that denaturation of a protein causes the increase in ASA with the decrease in volume (31), although relative contributions of four terms in Equation 3 to volume changes is difficult to access. An eventual positive or negative change in volume in a system of interest is a result of the delicate balance between these four terms.

*From the Acid-denatured β2-m to Native β2-m*—To investigate the effect of a possible residual structure in the acid-denatured β2-m, we compared the $\nu^\circ$ values of the different denatured species. We first obtained a $\nu^\circ$ of 0.636 ± 0.008 ml·g$^{-1}$ for the β2-m solution containing 6 mM HCl at pH 2.3 and 38 mM NaCl, which is similar to the $\nu^\circ$ of 0.640 ± 0.001 ml·g$^{-1}$ for the acid-denatured β2-m in 50 mM citrate buffer at pH 2.5 (Table 1). Adding 5.7 M Gdn-HCl to 50 mM citrate buffer at pH 2.5, the $\nu^\circ$ values of acid-induced unfolded β2-m further diminished to 0.620 ml·g$^{-1}$ (Table 1). This might imply the presence of residual structures in the acid-denatured β2-m as indicated by the ability to bind 1-anilino-8-naphthalenesulfonate (27) and by the fast relaxation rates of $^{15}$N with NMR spectroscopy (33). We suggest that the decrease in volume upon the addition of Gdn-HCl might result from disruption of the non-native cavities in the residual structure and from the increases in hydration, although there are possible changes in volume depending on the concentration of Gdn-HCl.

The structural transition of β2-m from the HCl-denatured (pH 2.3) to native (pH 7.0) species was accompanied by the increase in volume. This elevation is most likely because of the formation of internal cavities and a decrease in hydration despite reductions in excluded and thermal volumes. It is difficult, however, to distinguish between the contribution to changes in volume arising from the different pH values.

The $\nu^\circ$ of the native β2-m at pH 7.0 and 5 °C was rather low (0.652 ml·g$^{-1}$) as compared with $\nu^\circ$ at pH 7.0 and 20 °C and $\nu^\circ$ of other native proteins (Table 1) (18, 30). This can be explained by the positive value for the thermal expansibility of a protein, because thermal expansibility is defined by $(1/\nu^\circ)\ (\delta\nu^\circ/\delta T)_p$, where $T$ is temperature, and $p$ is pressure (18).

*From the Acid-denatured β2-m to Mature Amyloid Fibrils*—The formation of mature fibrils from monomers led to the increase in volume (Fig. 5*A*). This would be a balance between the increase in volume caused by the formation of cavities and the reduction in hydration and the decrease in volume because of reductions in thermal and excluded volumes. The magnitude of the change in volume was larger for the misfolding reaction (*i.e.* fibril formation) than folding reaction, by 0.025 ml·g$^{-1}$ (Fig. 5*A* and Table 1). The different extent of volumetric change between folding and misfolding implies that the difference in volume between amyloid fibrils and native species was caused by the formation of loosely packed amyloid fibrils.

This interpretation can be supported by our previous studies. A calorimetric study on the transitions of the amyloid fibrils and native β2-m to the unfolded β2-m suggested a similar extent of surface burial (similar $\Delta C_p$) in both conformational transitions and a lower level of internal packing (lower $\Delta H$) of amyloid fibrils than native monomers (5). Moreover, a high hydrostatic pressure study on amyloid fibrils of β2-m also indicated a lower level of internal packing of fibrils (3).

Interestingly, the $\nu^\circ$ of mature β2-m fibrils fragmented by sonication was indistinguishable from that of the original long fibrils (Table 1). This signifies that the increased ASA of terminal parts of fibrils on the shortening of mature fibrils was too small to affect the volumetric properties of mature fibrils, or was a result canceled out between four terms in Equation 3.

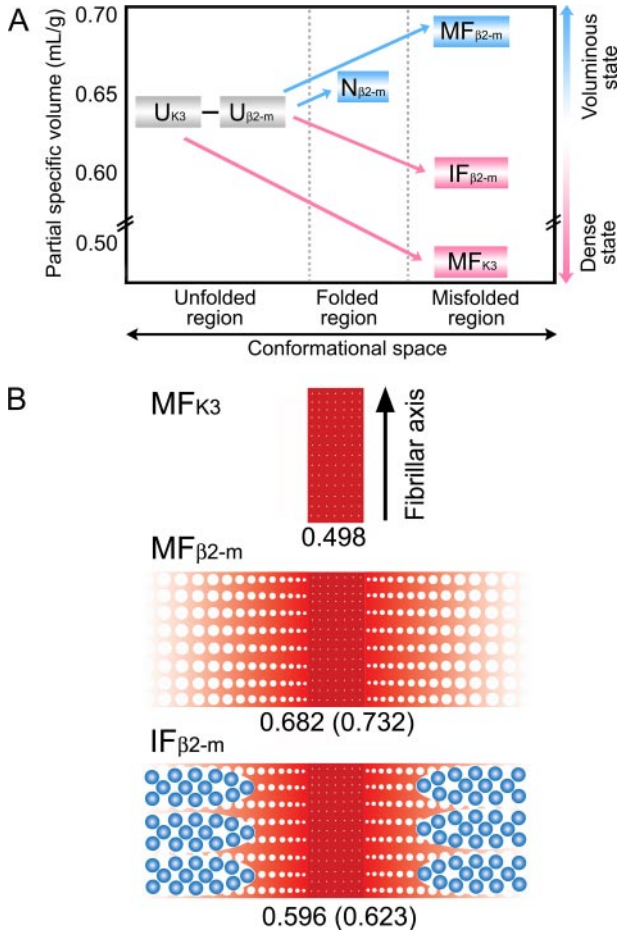


FIGURE 5. **Volumes of various conformational states and schematic models for distinct fibrillar conformations.** *A,* partial specific volume ($\nu^\circ$) of each conformation is shown as a function of conformational space, and boundaries of conformational regions are denoted with *dotted lines*. $U_{\beta2\text{-}m}$ exhibits acid-denatured β2-m, and $N_{\beta2\text{-}m}$ indicates native β2-m. $MF_{\beta2\text{-}m}$ exhibits mature amyloid fibrils of β2-m. Immature fibrils of β2-m are denoted as $IF_{\beta2\text{-}m}$. An amyloidogenic fragment of β2-m, K3 peptide, is shown as $U_{K3}$. $MF_{K3}$ indicates the mature fibrils of K3. The *tilted arrows* indicate directions of reactions for conformational transitions. *Magenta arrows* and *rectangles* represent decreases in volume following structural transition, and *blue arrows* and *rectangles* indicate increases in volume. The *short horizontal black line* indicates small differences in $\nu^\circ$ values between both structural states. *B,* proposed structures for the three types of fibrils are shown as side views along the fibril axis. The conformations of $MF_{K3}$, $MF_{\beta2\text{-}m}$, and $IF_{\beta2\text{-}m}$ are depicted. The *white spheres* of various sizes indicate internal cavities, and *blue circles* indicate water molecules. *Red rectangles* at the *center* show a compact core structure, and those outside the core structures indicate exhibit packing-defective regions. The values of $\nu^\circ$ in units of ml·g$^{-1}$ are denoted *below* the corresponding models, and the $\nu^\circ$ values for outside of the core structure are given in *parentheses*.

*From K3 Peptide to Mature Amyloid-like Fibrils*—The transition from the unfolded K3 monomer to the fibrils dropped significantly the $\nu^\circ$ (Fig. 5*A* and Table 1) in contrast to the transition of monomers to fibrils of β2-m. The negative volumetric change would be caused by the formation of remarkably tight packing inside the fibril. This coincides with our previous solid-state NMR study that suggested that the conformation of the K3 molecule in fibrils retains tight packing with adjacent K3 molecules (34). Moreover, the highly persistent protection profile of K3 fibrils, except the two residues of the N terminus revealed by hydrogen-deuterium exchange ($HD_{ex}$) experiments, suggests that most of residues of K3 constitute the core structure of the K3 fibrils (14).

Several other reports also pointed out that a tightly packed cross-β-structure, *i.e.* core structure, in the fibrils was made of short polypeptides (7–12, 25). It may also be conceivable that a water molecule is trapped in the cavity during the formation of fibrils, which cause a reduction in volume (35, 36). Taken together, mature K3 fibrils assume a highly packed conformation representative of a core structure of amyloid fibrils, although the effect of associations of fibrils on changes in volume is not considered here.

*From the Acid-denatured β2-m to Immature Amyloid-like Fibrils*—The changes in volume caused by the transition from monomers to immature fibrils were explored. Intriguingly, the $\nu^\circ$ of immature fibrils was lower than that of unfolded β2-m (Fig. 5*A* and Table 1). This decrease would result from the formation of a compact core structure in the center of immature fibrils rendering the outside of the core structure loosely/moderately packed and highly hydrated simultaneously. To investigate solvent accessibility, we further conducted Gdn-HCl-induced unfolding experiments for mature and immature fibrils (details are provided in supplemental Fig. S1). We found that mature fibrils were more stable than immature fibrils (supplemental Fig. S2), implying that immature fibrils are more prone to contact with the solvent than mature fibrils.

In addition, our recent work of $HD_{ex}$ for mature and immature fibrils reinforces this interpretation. Both fibrils formed at acidic pH showed distinct protection patterns (13, 14). Almost 80% of the entire sequence of β2-m was protected from $HD_{ex}$ in the mature fibrils involving the region corresponding to the core structure of K3 fibrils, whereas only 30% of the entire sequence was protected in the immature fibrils accommodating many residues of the core structure of K3 fibrils. Although the core structure of mature K3 fibrils was not exactly consistent with that of the mature and immature fibrils, the concept of a core structure at the center of mature and immature fibrils could still be valid.

*Simple Models for Various Fibrous Structures*—As indicated in Fig. 5*A*, an unstructured polypeptide folds to the native conformation with an increase in volume. However, misfolding of a random coil-like structure toward main-chain-dominated fibrous conformations can be followed by an increase or decrease in volume. To better understand various fibrils possessing distinct volumes and morphologies, we suggest concise models for three types of fibrous structures examined here with simple quantitative evaluation of $\nu^\circ$ (supplemental equation S1).

Mature fibrils of K3 would be comprised of a core structure with compact packing as evidenced by the $\nu^\circ$ of 0.498 ml g$^{-1}$ (Fig. 5*B*). The tight packing of K3 fibrils is a special case achieved only when all of the side chains can form ideal stabilizing interactions with their counterparts without any steric hindrance.

Mature fibrils of β2-m would accommodate a highly packed core structure that causes a decrease in volume, and the rest of the core structure mainly consists of solvent-inaccessible areas with extended hydrogen bonds and loose packing (Fig. 5*B*) that causes an increase in volume. Indeed, the estimated $\nu^\circ$ of the exterior region of the core structure ($\nu^\circ_{OUT}$) of mature β2-m fibrils was 0.732 ml g$^{-1}$ ( supplemental equation S1) and larger

than $\nu^{\circ}$ of native $\beta$2-m (0.652 ml $g^{-1}$) (Table 1), indicating a highly bulky state. Therefore, outside of the center can produce cavities, thereby rendering mature fibrils compressible and multiple structures called "polymorphism."

Likewise, the calculated $\nu^{\circ}_{OUT}$ of the immature fibrils was 0.623 ml $g^{-1}$, which is comparable with the unfolded state (Fig. 5*B* and Table 1). This value may be explained by much hydration and a small sparse area outside the core region with fewer hydrogen bonds (Fig. 5*B*). These volumetric features might endow immature fibrils with a thin curved conformation. It should be noted that the less volume changes of fibrillogenesis of the short TTR-(105–115) than that of the full-length TTR implying the core structure would support our model (21, 25).

In conclusion, taking the present and our previous results together, we suggested three concise and straightforward models illustrating the conformational states of the three fibrils at acidic pH. Although an evolutionally attained native structure is folded pursuing the optimal packing and burial of side chains (37), a main-chain-dominated structure of amyloid fibrils is formed with a lot of void spaces because of loose packing, which can subsequently trigger polymorphism of amyloid fibrils. This tunable volume change might signify that loosely packed parts of amyloid fibrils serve as its survival for responses of changes in ambient conditions such as robust folding pathways, in turn, and might mean an alternative evolutional selection as a rudimentary structure.

Finally, the comparisons between the partial volumes of the $\beta$2-m and K3 fibrils formed at acidic and neutral pH values would provide more detailed insights into structural models of amyloid fibrils, although we need further efforts of preparing well dispersed fibrils at neutral pH for ensuring the reliable and precise measurements of density.

*Acknowledgments—We thank Azusa Okamoto and Miyo Sakai for help with the Gdn-HCl-induced unfolding experiments and AUC measurements of the fibrils, respectively. We thank Shun-ichi Kidokoro (Nagaoka University of Technology) for technical support of densitometry.*

## REFERENCES

1. Jahn, T. R., and Radford, S. E. (2008) *Arch. Biochem. Biophys.* **469,** 100–117
2. Dobson, C. M. (2003) *Nature* **426,** 884–890
3. Chatani, E., Kato, M., Kawai, T., Naiki, H., and Goto, Y. (2005) *J. Mol. Biol.* **352,** 941–951
4. Chatani, E., Naiki, H., and Goto, Y. (2006) *J. Mol. Biol.* **359,** 1086–1096
5. Kardos, J., Yamamoto, K., Hasegawa, K., Naiki, H., and Goto, Y. (2004) *J. Biol. Chem.* **279,** 55308–55314
6. Fandrich, M., and Dobson, C. M. (2002) *EMBO J.* **21,** 5682–5690
7. Nelson, R., Sawaya, M. R., Balbirnie, M., Madsen, A. O., Riekel, C., Grothe, R., and Eisenberg, D. (2005) *Nature* **435,** 773–778
8. Sawaya, M. R., Sambashivan, S., Nelson, R., Ivanova, M. I., Sievers, S. A., Apostol, M. I., Thompson, M. J., Balbirnie, M., Wiltzius, J. J., McFarlane, H. T., Madsen, A. O., Riekel, C., and Eisenberg, D. (2007) *Nature* **447,** 453–457
9. Hiramatsu, H., Goto, Y., Naiki, H., and Kitagawa, T. (2004) *J. Am. Chem. Soc.* **126,** 3008–3009
10. Petkova, A. T., Ishii, Y., Balbach, J. J., Antzutkin, O. N., Leapman, R. D., Delaglio, F., and Tycko, R. (2002) *Proc. Natl. Acad. Sci. U. S. A.* **99,** 16742–16747
11. Jaroniec, C. P., MacPhee, C. E., Bajaj, V. S., McMahon, M. T., Dobson, C. M., and Griffin, R. G. (2004) *Proc. Natl. Acad. Sci. U. S. A.* **101,** 711–716
12. Luhrs, T., Ritter, C., Adrian, M., Riek-Loher, D., Bohrmann, B., Dobeli, H., Schubert, D., and Riek, R. (2005) *Proc. Natl. Acad. Sci. U. S. A.* **102,** 17342–17347
13. Hoshino, M., Katou, H., Hagihara, Y., Hasegawa, K., Naiki, H., and Goto, Y. (2002) *Nat. Struct. Biol.* **9,** 332–336
14. Yamaguchi, K., Katou, H., Hoshino, M., Hasegawa, K., Naiki, H., and Goto, Y. (2004) *J. Mol. Biol.* **338,** 559–571
15. Kihara, M., Chatani, E., Iwata, K., Yamamoto, K., Matsuura, T., Nakagawa, A., Naiki, H., and Goto, Y. (2006) *J. Biol. Chem.* **281,** 31061–31069
16. Kozhukh, G. V., Hagihara, Y., Kawakami, T., Hasegawa, K., Naiki, H., and Goto, Y. (2002) *J. Biol. Chem.* **277,** 1310–1315
17. Chalikian, T. V., Volker, J., Anafi, D., and Breslauer, K. J. (1997) *J. Mol. Biol.* **274,** 237–252
18. Gekko, K., Kimoto, A., and Kamiyama, T. (2003) *Biochemistry* **42,** 13746–13753
19. Chalikian, T. V. (2003) *Annu. Rev. Biophys. Biomol. Struct.* **32,** 207–235
20. Silva, J. L., Oliveira, A. C., Gomes, A. M., Lima, L. M., Mohana-Borges, R., Pacheco, A. B., and Foguel, D. (2002) *Biochim. Biophys. Acta* **1595,** 250–265
21. Foguel, D., Suarez, M. C., Ferrao-Gonzales, A. D., Porto, T. C., Palmieri, L., Einsiedler, C. M., Andrade, L. R., Lashuel, H. A., Lansbury, P. T., Kelly, J. W., and Silva, J. L. (2003) *Proc. Natl. Acad. Sci. U. S. A.* **100,** 9831–9836
22. Akasaka, K., Latif, A. R., Nakamura, A., Matsuo, K., Tachibana, H., and Gekko, K. (2007) *Biochemistry* **46,** 10444–10450
23. Smirnovas, V., Winter, R., Funck, T., and Dzwolak, W. (2005) *J. Phys. Chem. B.* **109,** 19043–19045
24. Smirnovas, V., Winter, R., Funck, T., and Dzwolak, W. (2006) *Chemphyschem.* **7,** 1046–1049
25. Dirix, C., Meersman, F., MacPhee, C. E., Dobson, C. M., and Heremans, K. (2005) *J. Mol. Biol.* **347,** 903–909
26. Hong, D. P., Gozu, M., Hasegawa, K., Naiki, H., and Goto, Y. (2002) *J. Biol. Chem.* **277,** 21554–21560
27. McParland, V. J., Kad, N. M., Kalverda, A. P., Brown, A., Kirwin-Jones, P., Hunter, M. G., Sunde, M., and Radford, S. E. (2000) *Biochemistry* **39,** 8735–8746
28. Yamaguchi, K., Takahashi, S., Kawai, T., Naiki, H., and Goto, Y. (2005) *J. Mol. Biol.* **352,** 952–960
29. Gekko, K., and Noguch, H. (1979) *J. Phys. Chem.* **83,** 2706–2714
30. Chalikian, T. V., Totrov, M., Abagyan, R., and Breslauer, K. J. (1996) *J. Mol. Biol.* **260,** 588–603
31. Sasahara, K., Sakurai, M., and Nitta, K. (1999) *J. Mol. Biol.* **291,** 693–701
32. Royer, C. A. (2002) *Biochim. Biophys. Acta* **1595,** 201–209
33. Platt, G. W., McParland, V. J., Kalverda, A. P., Homans, S. W., and Radford, S. E. (2005) *J. Mol. Biol.* **346,** 279–294
34. Iwata, K., Fujiwara, T., Matsuki, Y., Akutsu, H., Takahashi, S., Naiki, H., and Goto, Y. (2006) *Proc. Natl. Acad. Sci. U. S. A.* **103,** 18119–18124
35. Sasahara, K., Naiki, H., and Goto, Y. (2005) *J. Mol. Biol.* **352,** 700–711
36. Yamazaki, T., Blinov, N., Wishart, D., and Kovalenko, A. (2008) *Biophys. J.* **95,** 4540–4548
37. Dill, K. A., Bromberg, S., Yue, K., Fiebig, K. M., Yee, D. P., Thomas, P. D., and Chan, H. S. (1995) *Protein Sci.* **4,** 561–602
38. DeLano, W. L. (2002) *The PyMOL Molecular Graphics Syste*m, version 0.99rc6, DeLano Scientific, Palo Alto, CA

# A Comprehensive Model for Packing and Hydration for Amyloid Fibrils of $\beta_2$ -Microglobulin

Young-Ho Lee, Eri Chatani, Kenji Sasahara, Hironobu Naiki and Yuji Goto

*J. Biol. Chem. 2009, 284:2169-2175.*
*doi: 10.1074/jbc.M806939200 originally published online November 18, 2008*

---